American Journal of Pathology, Vol. 157, No. 1, July 2000

Disruption of Redox Homeostasis in Tumor Necrosis Factor-Induced Apoptosis in a Murine Hepatocyte Cell Line

Robert H. Pierce,* Jean S. Campbell,* Alyssa B. Stephenson,* Christopher C. Franklin,* Michelle Chaisson,* Martin Poot,* Terrance J. Kavanagh,† Peter S. Rabinovitch,* and Nelson Fausto*

From the Department of Pathology, the School of Medicine, and the Department of Environmental Health,† the School of Public Health, the University of Washington, Seattle, Washington*

Tumor necrosis factor (TNF) is a mediator of the acute phase response in the liver and can initiate proliferation and cause cell death in hepatocytes. We investigated the mechanisms by which TNF causes apoptosis in hepatocytes focusing on the role of oxidative stress, antioxidant defenses, and mitochondrial damage. The studies were conducted in cultured AML12 cells, a line of differentiated murine hepatocytes. As is the case for hepatocytes *in vivo*, AML12 cells were not sensitive to cell death by TNF alone, but died by apoptosis when exposed to TNF and a small dose of actinomycin D (Act D). Morphological signs of apoptosis were not detected until 6 hours after the treatment and by 18 hours ~50% of the cells had died. Exposure of the cells to TNF+Act D did not block NFκB nuclear translocation, DNA binding, or its overall transactivation capacity. Induction of apoptosis was characterized by oxidative stress indicated by the loss of NAD(P)H and glutathione followed by mitochondrial damage that included loss of mitochondrial membrane potential, inner membrane structural damage, and mitochondrial condensation. These changes coincided with cytochrome C release and the activation of caspases-8, -9, and -3. TNF-induced apoptosis was dependent on glutathione levels. In cells with decreased levels of glutathione, TNF by itself in the absence of transcriptional blocking acted as an apoptotic agent. Conversely, the antioxidant α-lipoic acid, that protected against the loss of glutathione in cells exposed to TNF+Act D completely prevented mitochondrial damage, caspase activation, cytochrome C release, and apoptosis. The results demonstrate that apoptosis induced by TNF+Act D in AML12 cells involves oxidative injury and mitochondrial damage. As injury was regulated to a larger extent by the glutathione content of the cells, we suggest that the combination of TNF+Act D causes apoptosis because Act D blocks the transcription of genes required for antioxidant defenses. *(Am J Pathol 2000, 157:221–236)*

Tumor necrosis factor (TNF) is a multifunctional cytokine that binds to two cell surface receptors,[1] tumor necrosis factor receptor type 1 and type 2 (TNFR1 and TNFR2, respectively). Most of the biological effects of TNF, including cell death,[2] are transduced through TNFR1, a receptor that contains a death domain near the intracellular C-terminus, similar to Fas (CD95 or Apo1). Clustering of the death domain of trimerized TNFR1 after ligand binding provides a docking site for TRADD (TNFR-associated death domain), an adapter protein[3] that can bind signaling molecules such as TRAF2 (TNFR-associated factor 2), RIP (receptor interacting protein), and FADD (Fas-associated death domain). Association of TRAF2 and RIP to the receptor results in the downstream activation of NFκB and AP-1, whereas FADD signaling initiates caspase activation.[4,5] Thus, TNFR1 signaling is bifurcated into two opposing pathways; one activating pro-inflammatory and mitogenic or survival responses while the other initiates programmed cell death.

In the liver, endotoxin (lipopolysaccharide)-mediated release of TNF triggers the up-regulation as well as down-regulation of acute phase response genes.[6] In addition to its role in inflammatory responses, TNF has other important effects in the liver. Recent studies from this and other laboratories[7,8] established that TNF is involved in the initiation of liver regeneration after partial hepatectomy or chemical injury through TNFR1 signaling.[9,10] In contrast, this cytokine acts as a cytotoxic agent in different types of liver injury such as in transplantation rejection and alcohol-induced hepatic disease,[11] although the precise mechanisms of TNF effects in these complex conditions are not entirely understood.[12] It has been reported that TNF by itself does not cause hepatocyte cell death.[13]

Supported by National Institutes of Health grants CA23226 and CA74131 (to N. F.), AG01751 (to P. S. R.), ES07032 (to T. J. K.), and CA 75316 (to C. C. F.). R. H. P. was supported by training grant ES07032 and the Irwin M. Arias Postdoctoral Research Fellowship from the American Liver Foundation. M. C. was supported by training grants CA09437 and GM0720.

Accepted for publication April 10, 2000.

Address reprint requests to Nelson Fausto, M.D., Department of Pathology, University of Washington, K-078 Health Sciences Building, Box 357705, Seattle, WA 98195. E-mail: nfausto@u.washington.edu.

However, sensitization to TNF cytotoxicity can be caused by drugs that directly block gene transcription or RNA translation or by less specific drugs that also inhibit gene transcription such as galactosamine and α-amanitine.[14]

Despite the extensive studies of TNF-mediated apoptosis in lymphocytes and other cells, there is relatively little specific information regarding the cell-death pathways activated by TNFR1 in hepatocytes. TNF causes cell death by necrosis or apoptosis depending on the intensity and duration of the stimulus and the overall metabolic status.[15] In cultured hepatocytes infected with an adenovirus expressing a dominant NFκB repressor, TNF-induced apoptosis and necrosis was preceded by the opening of high-conductance mitochondrial pores.[16] Although mitochondrial alterations may have been produced by reactive oxygen species (ROS), it remains controversial what role alterations in redox potential and cell antioxidant defenses may play in TNF-induced cell death. In L929 cells,[17,18] TNF toxicity was associated with ROS production while glutathione (γ-glutamylcysteinylglycine, GSH) acted as the main agent capable of reducing ROS levels. In contrast with these findings, Leist et al[13] reported that both oxidative stress and decreases in GSH occurred after morphological changes of apoptosis that were evident in hepatocytes exposed to TNF. Furthermore, Xu et al[19] also concluded that oxidative stress played no role in TNF-induced hepatocyte apoptosis because prevention of the up-regulation of antioxidant responses did not sensitize hepatocytes to TNF-induced cell death.

The interpretations of experiments to test the role of oxidant stress in TNF-mediated hepatocyte apoptosis are complicated by several factors. First, TNF may be capable of triggering apoptosis by more than one signaling pathway depending on variables such as the metabolic state of the cell and oxidative phosphorylation coupling.[20] For instance in HeLa cells, TNF given in combination with the protein synthesis inhibitor, emeline, activated two distinct apoptotic pathways, only one of which depended on the early release of mitochondrial ROS.[21] In addition, the intensity of the stimulus may determine the nature of the cellular response as excessive oxidative stress can block caspase activity by a direct effect on these proteases. Nonhepatic cells exposed to high concentrations of H_2O_2, as well as hepatocytes depleted of GSH, were resistant to apoptosis and had no detectable caspase-3 activity after treatment with agonist Fas antibodies.[22] Lastly, hepatocytes may differ from other cell types in their response to oxidative injury because they contain very high GSH levels.[23,24] It is likely that modulations of the cellular GSH content would have major effects on cell survival. All of these observations are consistent with a general model for mammalian cell apoptosis[25,26] that proposes that there are two main execution pathways: one involving mitochondrial damage (type II cells) and the other, a mitochondrial-independent pathway in which early caspase-8 activation is a major initiating event (type I cells). We hypothesized that because of the abundance of mitochondria, high oxidative phosphorylation rates, and the high levels of GSH in hepatocytes, TNF-induced apoptosis in these cells may be highly dependent on mitochondrial functional and structural integrity.

In this report, we focused our analysis of the mechanisms mediating TNF-induced apoptosis in hepatocytes on the role of oxidative stress, antioxidant defenses, and mitochondrial damage. The studies were conducted in cultured AML12 hepatocytes, which, as is the case for murine hepatocytes *in vivo*,[13] are not sensitive to cell killing by TNF, but die by apoptosis when exposed to TNF and in the presence of a small dose of actinomycin D (Act D). The results obtained indicate that the balance between mitochondrial oxidant stress and endogenous antioxidant defense mechanisms involving GSH plays a determinant role in TNF-induced apoptosis in hepatocytes.

Materials and Methods

Tissue Culture

AML12 hepatocytes, a well-differentiated, nontransformed murine hepatocyte cell line derived from transforming growth factor-α (TGF-α) transgenic mice were used for all experiments.[27] In brief, AML12 cells were maintained in Dulbecco's minimal essential medium/F12 (Life Technologies Inc., Grand Island, NY) with 10% fetal bovine serum (Hyclone, Logan, UT), 5 μg/ml insulin, 5 μg/ml transferrin, 5 ng/ml selenium (ITS Premix, Collaborative Biomedical Products (Bedford, MA)), 50 μg/ml gentamicin, and 0.1 μmol/L dexamethasone. Cultures were grown at 37°C in a humidified 6% CO_2 atmosphere, fed approximately every 72 hours, and passaged at ~80 to 90% confluence.

Chemicals and Reagents

Act D, buthionine sulfoximine (BSO), diethyl maleate (DEM), dexamethasome, and menadione (MEN) were purchased through Sigma Chemical Co. (St. Louis, MO). Acetyl-Asp(OMe)-Glu(OMe)-Val-Asp(OMe)-aminomethylcoumarin (DEVD-AMC), acetyl-Ilu(OMe)-Glu(OMe)-Thr-Asp(OMe)-aminomethylcoumarin (IETD-AMC), and acetyl-Leu(OMe)-Glu(OMe)-His-Asp(OMe)-aminomethylcoumarin (LEHD-AMC) were purchased from Biomol (Plymouth Meeting, PA) whereas benzyloxycarbonyl-Val-Ala-Asp(OMe)-fluoromethylketone (zVAD-FMK) and α-lipoic (α-LA) acid were obtained from Bachem (Torrance, CA) or Calbiochem (La Jolla, CA), respectively. Mitotracker green (MTG), chloromethyl-x-rosamine (CMX), nonyl acridine orange (NAO), monochlorobimane (MCB), and monobromobimane were purchased from Molecular Probes (Eugene, OR). Recombinant murine TNF was purchased from R&D Systems (Minneapolis, MN). Antibodies to p65 (sc-372-G), and caspase-8 (Mch 5, sc-6134) were purchased from Santa Cruz Biotechnology (Santa Cruz, CA), whereas anti-caspase-3 antibodies (C76920) were purchased from Pharmingen (San Diego, CA). Horseradish peroxidase-conjugated anti-mouse secondary antibody was purchased from Amersham Pharmacia Biotech (NA 931; Piscataway, NJ) and the horseradish peroxidase-

conjugated anti-goat secondary antibody was purchased from Santa Cruz (sc-2020).

Induction of Apoptosis with TNF+Act D

AML12 cells were trypsinized, plated, and allowed to adhere and grow overnight. At 90 to 95% confluence, the cells were pretreated with either 200 nmol/L (250 ng/ml) Act D or phosphate-buffered saline (PBS) in fresh medium for 30 minutes followed by either 20 ng/ml TNF (dissolved in PBS containing 1.0% bovine serum albumin, fraction V, to a stock concentration of 2.0 μg/ml) or PBS control. Treatment of cells plated at lower densities resulted in much more rapid kinetics of apoptosis than cultures plated at 90 to 95% confluency. *In vivo* induction of hepatocyte apoptosis was done as described by Leist et al.[13] For these experiments C57BL/6 mice received either TNF (3.3 μg/kg) or Act D (800 μg/kg) alone or in combination. The Act D injection was given 15 minutes before the TNF injection and the mice were killed 3 to 6 hours after the TNF injection. Livers were harvested, fixed in 10% buffered formalin, processed, and stained with hematoxylin and eosin. Apoptosis was assessed morphologically.

Pharmacological Activation and Inhibition of AML12 Apoptosis

AML12 cells were pretreated with 100 μmol/L zVAD-FMK (3 hours pretreatment) or 1 mmol/L α-LA acid (60 minutes pretreatment) followed by treatment with Act D and then TNF as described above. To alter intracellular GSH content, AML12 cells were pretreated with BSO (1 mmol/L dissolved in AML12 media) for 60 minutes to block *de novo* GSH synthesis then 0.8 mmol/L DEM (made fresh in AML12 media) to acutely deplete GSH. For experiments with menadione, AML12 cells were pretreated for 3 hours at a concentration of 100 μmol/L, followed by treatment with Act D or Act D with α-LA (1 mmol/L) for 9 hours.

Electrophoretic Mobility Shift Assay (EMSA)

AML12 cells were lysed and nuclei were extracted as reported previously.[28] In brief, 5 μg of nuclear protein were incubated at room temperature for 30 minutes with 0.2 ng of ^{32}P-end-labeled double-stranded oligonucleotide (NFκB binding site from the class 1 major histocompatibility enhancer element H2K), followed by electrophoresis through a 5% polyacrylamide Tris-glycine-ethylenediaminetetraacetic acid (EDTA) gel. Gels were dried under a vacuum and exposed overnight to Kodak X-AR film (Eastman Kodak Co., Rochester, NY) at −80°C with an intensifying screen.

Immunoblot Analysis

AML12 cells were rinsed in PBS and lysed in a 1% Triton X-100 buffer containing 50 mmol/L Tris-HCl, pH 7.4, 50 mmol/L β-glycerophosphate, 150 mmol/L NaCl, 2 mmol/L EDTA, 1 mmol/L Na_3VO_4, 1 mmol/L benzamidine, 1 mmol/L dithiothreitol, 10 μg/ml leupeptin, 10 μg/ml pepstatin A, 10 μg/ml aprotinin, 0.5 mmol/L 4-(2-aminoethyl)-benzenesulfonyl fluoride hydrochlorine (ICN Biomedicals, Irvine, CA), and 10% glycerol. Protein quantitation was performed using Bradford reagent (Bio-Rad, Hercules, CA) and 50 μg of total protein lysate was subjected to sodium dodecyl sulfate-polyacrylamide gel electrophoresis and transferred to polyvinylidene difluoride (Millipore, Bedford, MA). Immunoblot analysis of nuclear protein was performed using 10 μg of protein isolated as described above. Release of cytochrome C into the cytosol was determined by immunoblot as described by Ghibelli et al[29] using a mouse monoclonal anti-cytochrome C antibody (PharMingen, La Jolla, CA). Membranes were blocked in Tris-buffered saline with 0.1% Tween 20 containing 5% milk (blotting grade; BioRad, Hercules, CA) at 4°C and incubated with primary antibodies at the following dilutions: p65, 1:2,000; Mch5, 1:1,000; caspase-3, 1:1,000; and cytochrome C, 1:1,000, in 0.5% milk in Tris-buffered saline with 0.1% Tween 20 for 1 to 2 hours. The appropriate secondary antibodies were added for 2 to 3 hours in 0.5% milk in Tris-buffered saline with 0.1% Tween 20 and antigen-antibody complexes were detected with enhanced chemiluminescent reagents purchased from either Dupont-New England Nuclear (Boston, MA) or Pierce (Rockford, IL).

Transient Transfections and Luciferase Assays

AML12 cells were co-transfected with a 4× NFκB luciferase reporter gene[30] and a CMV β-galactosidase gene using lipofectamine (Life Technologies, Inc.) following the manufacturer's protocol in a 2:1 ratio (1.5 μg total DNA). The transfection medium containing DNA/lipofectamine was removed after 5 hours and cells were treated immediately. Cells were harvested 14 hours after transfection and processed for luciferase and β-galactosidase assays using the Dual Light System (Tropix, Bedford, MA), according to the manufacturer's instructions. This system allows for sequential determinations of luciferase and β-galactosidase on the same experimental sample.

Flow Cytometric Detection of Cellular Redox State and Mitochondrial Alterations

Flow cytometry was performed on a Coulter Epics Elite (Coulter Electronics, Hialeah, FL) using time-resolved dual laser excitation: 15 mW 488 argon (nondelayed) and 20 mW UV argon (delayed, 40 μS). Fluorescence measurements were done with the following dyes as previously described:[31–33] MCB and monobromobimane to measure GSH and reduced cellular thiols, respectively; CMX to measure mitochondrial membrane potential; MTG to measure mitochondrial mass; NAO to measure cardiolipin content; and dichloromethyl-x-rosamine (H2-CMXROS), a mitochondrial selective dye that becomes fluorescent when oxidized, to measure mitochondrial ROS. UV excited blue autofluorescence was used to

measure reduced NAD, designated NADPH to represent contributions by both NADH and NADPH. For each sample, 488-nm forward light scatter to determine cell size and UV laser right-angle light scatter were measured. Fluorescent intensity was displayed on a logarithmic scale.

AML12 cells were cultured in 6-well tissue culture plates. The culture supernatant was pooled with the attached cells, which were harvested with trypsin/EDTA (Life Technologies, Inc.). An aliquot of cells was added to a tube containing an equal volume of 2× solution of the indicated dyes in cell culture medium and incubated with occasional mixing for 30 minutes in the tissue culture incubator. The cells were then placed on ice in the dark and run on the flow cytometer. At least 15,000 events were recorded per sample.

Analysis of flow cytometric experiments was performed using the software package MPLUS (Phoenix Flow Systems, San Diego, CA). To help eliminate debris, a UV-side scatter *versus* 488-forward scatter gate determined by analysis of the untreated control samples was applied. Analytic (nonexclusionary) gates drawn around the entire population or distinct subpopulations were used to determine the median fluorescence values and percentage of cells associated with those groups. Identical gates were used for all comparisons.

DAPI Fluorescence

Trypsinized cells were fixed in 70% ETOH, centrifuged at 50 to 80 × *g* for 5 minutes and resuspended in a solution containing 0.5% Nonidet P-40 and 10 μg/ml DAPI. Apoptotic nuclear morphology was assessed as described by Hotz et al[34] on 200 cells per experimental point and each point was determined in triplicate.

Confocal Laser Microscopy

AML12 cells were cultured on 2-well coverslip chambers (Nunc Inc., Bountiful, UT) and after treatment, the cultures were stained with CMXROS and MTG for 15 minutes at 37°C. Cells were scanned with an ACAS Ultima Confocal Laser Cytometer (Meridian Instruments, Okemos, MI) and confocal images were acquired using a 60× oil objective (NA = 1.3). Fields were first scanned for fluorescence from the mitochondrial stains, and then the NAD(P)H fluorescence images were collected from the same field. Images are displayed as composite images (red, green, blue) using Adobe Photoshop (Adobe Systems, Inc., San Jose, CA).

Transmission Electron Microscopy

Cells harvested by trypsinization were fixed at room temperature overnight in one-half strength Karnovsky's fixative. Cells were then rinsed in 0.1 mol/L phosphate buffer, postfixed in a 2% buffered osmium tetroxide solution, followed by dehydration through a graded series of ethanol solutions. Cells were rinsed with propylene oxide and infiltrated with 1:1 mix of PolyBed (Polysciences, Warrington, PA)/propylene oxide followed by 100% PolyBed. Cells were then embedded in PolyBed and polymerized at 60°C overnight. Sections (70 to 90 nm) were stained with saturated solutions of uranyl acetate and lead tartrate and micrographs were taken on a Philips 410 transmission electron microscope (FEI Co., Hillsboro, OR).

Detection of Caspase Activity

Caspase-8, caspase-9, and caspase-3 activities were measured using the substrates, IETD-AMC, LEHD-AMC, and DEVD-AMC (Biomol), respectively. Cells were harvested and lysed in the Triton X-100 lysis buffer described above. Protein lysate (50 μg) was incubated for 30 minutes at 37°C in a caspase assay buffer (50 mmol/L Hepes, pH 7.4, 100 mmol/L NaCl, 2 mmol/L EDTA, 10% sucrose, 0.1% CHAPS, (3-[(3-cholamidopropyl)dimethyl ammonio]-1-propanesulfonate (Meriden, CN) 10 mmol/L dithiothreitol) containing 10 μmol/L of each peptide-aminomethylcoumarin substrate. Enzymatic assays and aminomethylcoumarin standard curves were carried out in duplicates using a fluorescent plate reader (Packard Instruments, Meriden, CT) with excitation and emission wavelengths of 360 nm and 460 nm, respectively. Fluorescence of the substrate blank was subtracted as background in each assay. Data analysis was performed using Packard's I-Smart software.

Statistical Analysis

Statview 4.5 (Abacus Concepts, Berkeley, CA) was used to perform the statistical analyses. For comparisons between means of multiple groups multifactorial analysis of variance with a Fischer's least significant difference was used. To assess the interaction between variables, 2-factor analysis of variance was used. The degree of correlation between flow cytometric parameters was assessed using a simple regression analysis. For all tests, $P < 0.05$ was accepted as significant.

Results

To study TNF-induced apoptosis in murine hepatocytes, we first determined whether TNF alone or in conjunction with Act D would cause apoptosis of mouse hepatocytes *in vivo*. In agreement with the data of Leist et al,[13] histological analysis of the liver of mice showed that neither TNF nor Act D by themselves caused cell death but the combination of TNF+Act D was highly apoptotic (data not shown). In livers of mice injected with TNF+Act D there were large numbers of apoptotic hepatocytes showing typical chromatin condensation in the nuclear periphery as well as the presence of apoptotic bodies and destruction of hepatic cords.

Similar to murine hepatocytes *in vivo*, AML12 hepatocytes in cultures were also insensitive to TNF-induced killing but died by apoptosis after exposure to TNF+Act D. AML12 cells were divided into four groups: 1) pretreated with Act D (200 μmol/L) for 30 minutes followed

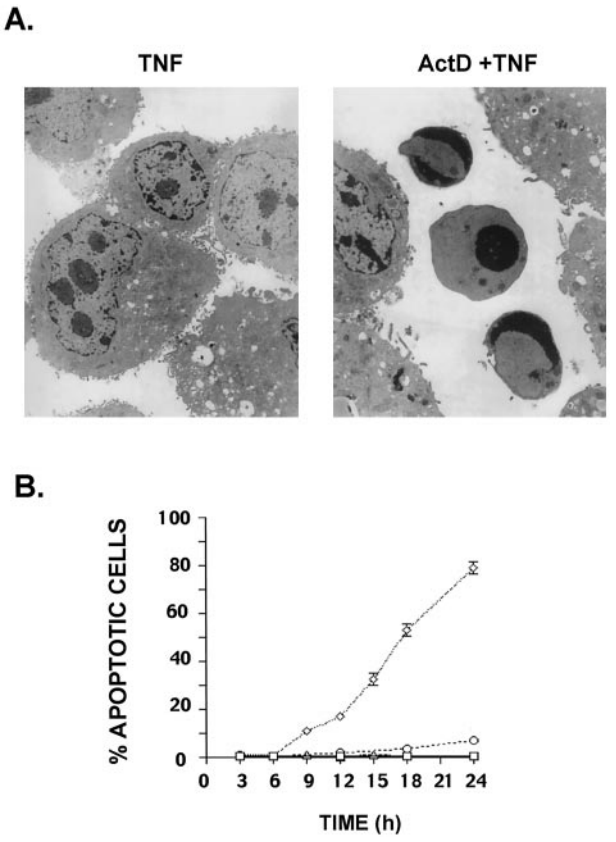

Figure 1. Apoptosis in AML12 cells exposed to TNF+Act D. Cells were pretreated with Act D (200 nmol/L) or saline (control) for 30 minutes and then TNF (20ng/ml) or PBS was added for the indicated times. **A:** After 15 hours of the indicated treatment, the cells were fixed and prepared for transmission electron microscopy as described in Materials and Methods (left panel, TNF treated; right panel, TNF+Act D). **B:** Cells were fixed in 70% ETOH at the indicated time points and apoptotic nuclear morphology was visualized by DAPI fluorescence. The percentage of apoptotic cells was measured in four treatment groups: saline and PBS (**squares**), Act D alone (**circles**), TNF alone (**triangles**), or TNF+Act D (**diamonds**). Each point was determined in triplicate and the error bars represent SEM. The results are representative of at least five independent experiments.

by addition of 20 ng/ml of TNF; 2) treated with TNF only; 3) treated with Act D only; and 4) left untreated for the duration of the experiment. Apoptosis was assessed between 3 and 24 hours by various procedures: light and electron microscopy, DAPI staining, detection of a subG1 peak by flow cytometry, and terminal dUTP nick-end labeling assays. The results obtained by these various methods were consistent and only electron microscopy and DAPI fluorescence analysis are presented (Figure 1, A and B). Untreated cells or cells treated with either TNF or Act D alone exhibited no morphological signs of apoptosis when analyzed by electron microscopy. In marked contrast, cells treated with TNF+Act D showed typical chromatin condensation (Figure 1A) as well as apoptotic bodies, in a pattern similar to that observed in livers of mice injected with the same drug combination. Microscopic analysis by DAPI fluorescence showed that changes in nuclear morphology characteristic of apoptosis were negligible (<1%) in cells exposed to TNF alone or left untreated. In cells exposed to TNF+Act D there was no detectable effect on DAPI fluorescence within the first 6 hours after exposure. However, after 24 hours of exposure ~80% of the cells were dead with characteristic morphological changes of apoptosis (Figure 1B). Approximately 50% of the cells exposed to TNF+Act D were apoptotic by 18 hours whereas only 5% of the cells showed morphological changes after 18 hours of exposure to Act D alone.

NFκB Binding and Transactivation Activity after TNF+Act D Treatment

In hepatocytes and other cell types, inhibition of NFκB activation sensitizes cells to TNF-induced apoptosis.[16,35–39] Microinjection of IκB protein or p65(rel A) antibodies into AML12 cells as well as transfection of the cells with an IκB superrepressor gene, conditions in which NFκB is made functionally inactive, sensitizes AML12 hepatocytes to apoptosis after TNF treatment.[40,41] To determine whether Act D sensitizes AML12 cells to TNF-induced apoptosis by inhibiting NFκB activity, p65 translocation to the nucleus and NFκB DNA binding activity were analyzed by immunoblot and EMSA, respectively. TNF activation of NFκB is generally accompanied by a transient increase of NFκB (p65/p50) in the nucleus.[42] Western blot analysis presented in Figure 2A shows an increase of nuclear p65 levels in cells treated for 30 minutes with either TNF alone or TNF+Act D. After 2 hours there was still no difference in nuclear p65 levels between these two treatment groups (data not shown). To determine whether TNF+Act D treatment blocked NFκB binding, nuclear extracts were prepared from cells treated with Act D or TNF alone or together. NFκB DNA binding determined by EMSA was increased in cells treated with TNF for 30 minutes. The apoptosis-inducing combination of TNF+Act D did not inhibit NFκB binding measured after 30 minutes (Figure 2B) or 2 hours (data not shown) of TNF treatment. Signal transducers and activators of transcription 3 (STAT3) binding also increased after TNF treatment in AML12 cells and this binding was not inhibited by Act D pretreatment (data not shown). Activation of STAT3 is linked to NFκB activity through interleukin-6, a NFκB target gene and a potent transactivator of STAT3.[43–45]

NFκB EMSA analysis measures the translocation of the heterodimer to the nucleus and its binding to DNA. However, DNA binding may not accurately reflect NFκB transactivation activity. To determine whether NFκB transactivation capacity was decreased in cells pretreated with Act D, cells transiently transfected with a NFκB-luciferase reporter construct were pretreated for 30 minutes with Act D followed by a 9-hour exposure to TNF. NFκB transcriptional activity was unaltered in cells exposed to Act D alone whereas TNF treatment alone caused a sevenfold to eightfold increase in reporter gene activity relative to the activity of untreated cells (Figure 2C). This increase was not blocked in cells pretreated with Act D and subsequently exposed to TNF. Cells were cotransfected with a CMV driven β-galactosidase gene to serve as a control in these experiments. β-galactosidase activity was increased by 50 to 70% in all treatment groups relative to

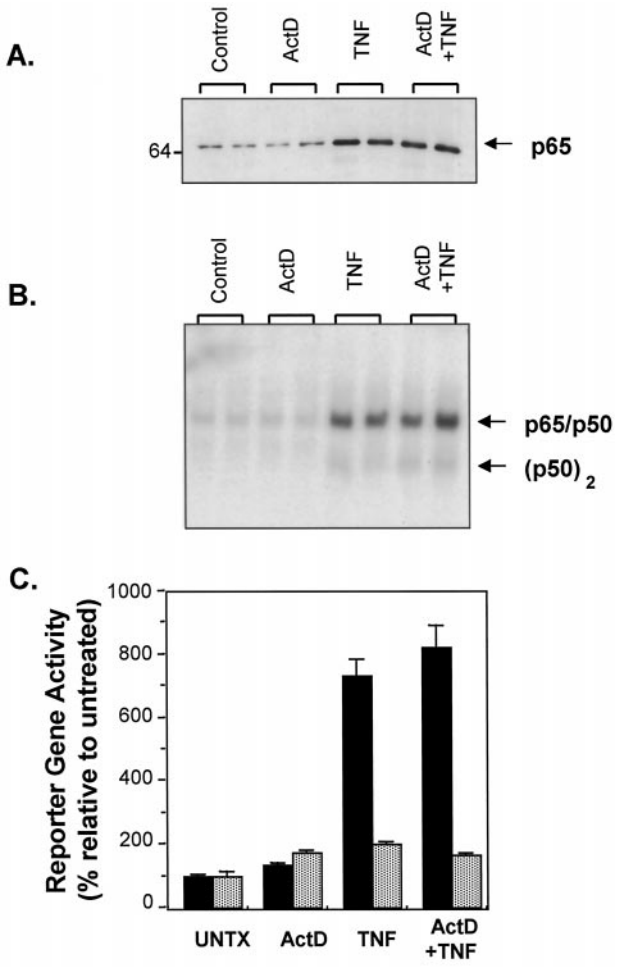

Figure 2. Analysis of NFκB activation and transcriptional activity. **A** and **B:** Cells were pretreated for 30 minutes with Act D (200 nmol/L) or saline followed by TNF (20 ng/ml). Nuclear extracts were prepared as described in Materials and Methods. **A:** Nuclear accumulation of p65 was assessed by immunoblot analysis. Duplicate samples of nuclear extracts (10 μg) were analyzed for p65 protein after 30 minutes of TNF treatment. Molecular weight markers indicated on the left. **B:** EMSA for NFκB after 30 minutes of exposure to TNF were carried out as described in Materials and Methods. The upper band (NFκB) consists of the p65/p50 heterodimer; the lower band is the p50/p50 homodimer. Duplicate samples are shown. These results are representative of three independent experiments. **C:** NFκB activation after TNF+Act D treatment was analyzed by a luciferase reporter gene. Cells were cotransfected with CMV β-galactosidase and NFκB-driven luciferase reporter constructs using lipofectamine, as described in Materials and Methods. After 5 hours, TNF+Act D was added for 9 hours as described in Materials and Methods. Cells were harvested and aliquots of protein lysate were assayed sequentially for both luciferase (**black bars**) and β-galactosidase activity (**stippled bars**). The bars depict SEM from six independent samples relative to untreated cells (UNTX).

untreated cells. Together, these results show that exposure of cells to the apoptotic-inducing combination of TNF+Act D did not block NFκB nuclear translocation or DNA binding or transactivation capacity. However, the luciferase transactivation assay may overestimate biologically relevant NFκB transcriptional activity and not account for the possible inhibition of transactivation of individual genes. Indeed, IκBα mRNA, the product of a gene transactivated by NFκB, was decreased after 6 hours of exposure to TNF + Act D compared to TNF alone (data not shown).

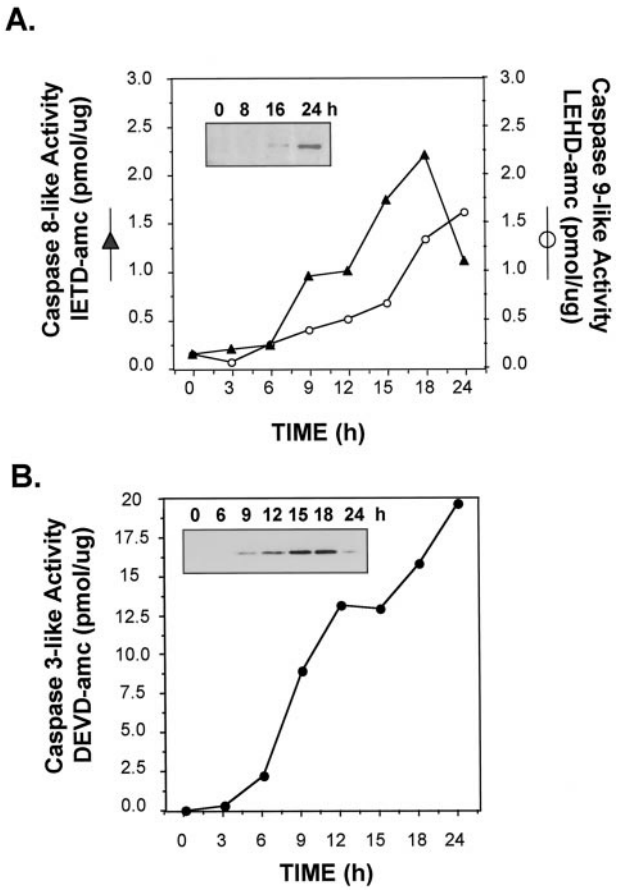

Figure 3. Activation of caspase-3, -8, and -9 in AML12 cells treated with TNF+Act D. Cells were pretreated for 30 minutes with Act D (200 nmol/L) followed by stimulation with TNF (20 ng/ml). Cellular extracts were prepared and protein concentrations were determined as described in Materials and Methods. **A:** Caspase-8 and caspase-9 activities were determined on protein lysates using IETD-AMC (**filled triangles**) and LEHD-AMC (**open circles**), respectively. **Inset:** Immunoblot analysis on the appearance of the cleaved, active form of caspase-8 at the indicated times after treatment of TNF+Act D. **B:** Caspase-3 activity was determined on protein lysates using DEVD-AMC. **Inset:** Immunoblot analysis on the appearance of the cleaved, active form of caspase-3 at the indicated times after treatment with TNF+Act D. Each data point represents the average of duplicate samples. These data are representative of three independent experiments.

Caspase Activation during TNF-Induced Apoptosis

Caspase activation is a characteristic feature of the apoptotic process. To determine the kinetics of caspase activation during TNF+Act D-induced apoptosis, caspase-3, -8, and -9 activities were measured using fluorogenic substrates after exposure of AML12 cells to TNF+Act D. No significant activation of caspase-8 and -9 measured, respectively, as IETD and LEHD cleavage activities was detected before 6 hours of treatment of TNF+Act D (Figure 3A). Caspase-3 activity (DEVD), on the other hand, was detectable between 3 and 6 hours. To directly investigate the activation of the caspases, immunoblot analysis was performed to detect the active, cleaved forms of caspase-8 (inset in Figure 3A) and caspase-3 (inset in Figure 3B). The caspase-8 cleavage product was not detectable until 16 hours after TNF+Act D treatment and was greatly increased by 24 hours. The

cleaved, active form of caspase-3 was detected by 9 hours and was maximal by 15 to 18 hours. Cells exposed to TNF or Act D as single agents had no increase in the activity of caspases-3, -8, and -9 (data not shown). These data indicate that TNF-induced caspase activation in hepatocytes is not a direct effect of the cytokine but is detected during apoptosis caused by treatment of cells with TNF in conjunction with Act D.

NAD(P)H and GSH Levels Decrease in Hepatocytes Treated with TNF+Act D

TNF has been shown to induce mitochondrial ROS production in cultured hepatocytes as well as in the liver *in vivo*.[24] NADH and NADPH are major sources of cellular reducing equivalents which are, in part, components of antioxidant defense mechanisms that prevent damage from oxidative stress. The liver is the main producer of GSH, a tripeptide thiol, which, among other functions, scavenges free radicals and helps to maintain protein thiol redox status.[23,46] To determine whether treatment of AML12 cells with TNF+Act D causes a change in reducing equivalents, NAD(P)H and GSH were measured by flow cytometry in cells at various times after treatment. Figure 4A shows a NAD(P)H histogram comparing untreated cells to cells exposed to TNF+Act D for 12 hours. It is clear from the histogram that the treatment caused a dramatic decrease in the number of cells containing normal levels of NAD(P)H. Quantification of these changes is shown in Figure 4B. This figure was constructed from histograms similar to that shown in Figure 4A for cells exposed to TNF+Act D for 3 to 15 hours. A reduction in NAD(P)H levels was first detected at 3 hours and by 6 hours there was a statistically significant difference in NAD(P)H between untreated cells and cells exposed to TNF+Act D. By 15 hours of treatment, NAD(P)H levels had decreased by 50% (Figure 4B) and only 25% of the cells retained normal NAD(P)H levels (data not shown). Cellular GSH levels also decreased with kinetics similar to that of NAD(P)H in response to the TNF+Act D treatment (Figure 4B). Measurements of total reduced thiols in these cells by flow cytometry using monobromobimane fluorescence (not shown) demonstrated that total reduced thiols also decreased after TNF+Act D treatment in a manner similar to that of GSH. This is to be expected because GSH is present in large amounts in hepatocytes and is the main component of the total reduced thiol fraction of these cells.

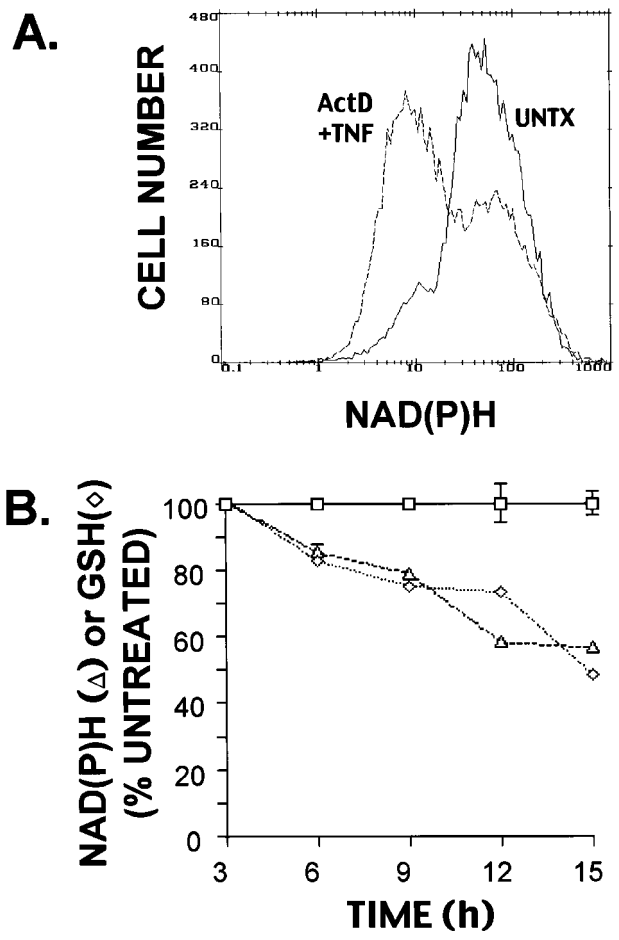

Figure 4. Loss of NAD(P)H and GSH levels in cells undergoing apoptosis. Cells were treated with TNF+Act D or saline (UNTX) and harvested for flow cytometry as described in Materials and Methods. **A:** Univariant NAD(P)H histogram for UNTX cells and cells treated for 12 hours with TNF+Act D. Total cellular reduced NAD (labeled as NAD(P)H to reflect contributions of from both NADH and NADPH) was measured as UV-excited blue autofluorescence (450 nm). Note that median fluorescence as well as the percent of the cells that remain within normal range can be derived from these curves. **B:** Time course of the coordinate loss of NAD(P)H and GSH is shown. NAD(P)H was determined by UV-excited blue fluorescence at 450 nm. GSH was measured by staining with MCB. Data points represent the percentage of cells that retain normal NAD(P)H (**open triangles**) or GSH (**open diamonds**) levels relative to the corresponding values obtained for the untreated samples (**open squares**). Error bars represent SEM from three independent samples. These data are representative of at least three independent experiments.

Mitochondrial Alterations in TNF-Induced Apoptosis

To determine whether the decrease in reducing equivalents caused by TNF+Act D treatment involves loss of mitochondrial function or damage to mitochondrial structure, mitochondrial transmembrane potential ($\Delta\psi$m) was measured by flow cytometry using the fluorescent dye CMX. A bivariate plot of the transmembrane potential and NAD(P)H shows that a large proportion of cells exposed to TNF+Act D for 12 hours had reduced transmembrane potential and lower NAD(P)H levels compared to untreated cells (Figure 5A). The relationship between these parameters is linear; simple regression analysis (not shown) demonstrated that there is a highly significant correlation ($R^2 = 0.72$; $P < 0.0001$) between the decrease in $\Delta\Psi$m and NAD(P)H loss. A reduction in $\Delta\Psi$m was detectable between 3 and 6 hours after exposure of cells to TNF+Act D and steadily declined over time, dropping to ~65% of control after 15 hours of treatment (Figure 5C).

Cardiolipin is a mitochondrial inner membrane phospholipid which plays a major role in maintenance of membrane proteins including cytochrome C.[47,48] Structural defects of cardiolipin-containing mitochondrial mem-

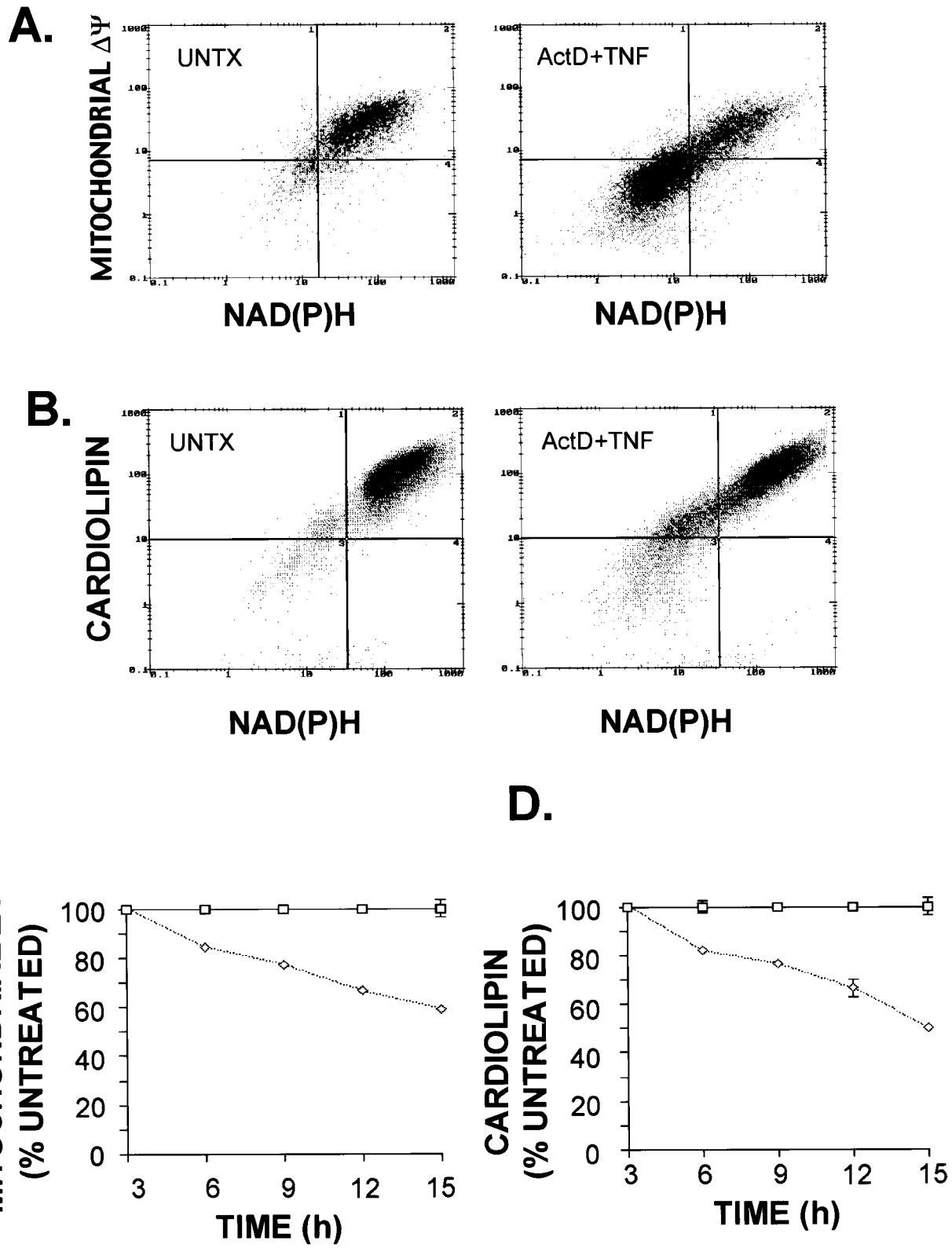

Figure 5. Loss of mitochondrial membrane potential and mitochondrial cardiolipin in cells undergoing apoptosis. Cells were treated with TNF+Act D and harvested for flow cytometry analysis as described in Materials and Methods. **A:** Bivariate dot-plots of membrane potential ($\Delta\Psi_m$, measured by CMX staining) and NAD(P)H from untreated (UNTX) cultures and cultures treated for 12 hours with TNF+Act D. **B:** Bivariate dot-plots of cardiolipin content (NAO staining) and NAD(P)H from untreated (UNTX) cultures and cultures treated for 12 hours with TNF+Act D. **C** and **D:** Time course of the progressive loss of mitochondrial membrane potential (**C**) and cardiolipin content (**D**) after TNF+Act D exposure. The exposure time is indicated on the abscissa. Data points represent the mean of the percent of cells that retain normal mitochondrial membrane potential (**C**) or cardiolipin content (**D**). Levels were calculated relative to untreated samples (**open squares**). Error bars represent SEM from three independent samples. These data are representative of at least three independent experiments.

branes caused by lipid peroxidation[49–51] can be assessed by staining with the fluorescent dye NAO. To determine whether cardiolipin staining was altered in TNF-induced apoptosis, cells were exposed to TNF+Act D for 12 hours and analyzed by flow cytometry for cardiolipin and NAD(P)H (Figure 5B). A bivariate plot of cardiolipin (NAO fluorescence) and NAD(P)H demonstrated that TNF+Act D exposure increased the proportion of cells with reduced cardiolipin and lower NAD(P)H content. There was a high degree of correlation between these changes ($R^2 = 0.88$; $P > 0.0001$). Loss of NAO fluorescence indicative of mitochondrial membrane damage progressively increased in cells exposed to TNF+Act D over time (Figure 5D) in a similar way as the changes in $\Delta\psi$m.

Mancini et al[52] reported that apoptosis of human colon carcinoma cells was associated with proliferation of condensed mitochondria with diminished transmembrane potential. These mitochondrial changes followed cell cycle arrest and preceded apoptosis. Electron microscopy and flow cytometry were used to determine whether similar changes occurred in AML12 cells during TNF+Act D inducing apoptosis. AML12 hepatocytes treated for 12 hours with TNF+Act D showed a decrease in mitochondrial volume, increased electron density, and an obscuring of cristae structure (Figure 6A). These mitochondria resembled mitochondrial condensation during apoptosis in other systems variably referred to as condensation, hypercondensation, or ultracondensation.[52–54] Compared to untreated cells, TNF+Act D did not cause a readily demonstrable mitochondrial swelling (typical of necrosis or the later stages of apoptosis) or an increase in mitochondrial number.

The dye MTG can be used to quantitate total cellular mitochondrial mass.[55] A bivariate plot of MTG fluorescence and NAD(P)H in untreated cells and in cells exposed to TNF+Act D is shown in Figure 6B. Most of the untreated cells fit into a population with high NAD(P)H content and variable MTG fluorescence. However in cells treated with TNF+Act D, a small proportion of the cells had lower NAD(P)H levels and high MTG fluorescence. This population of cells increased by twofold to threefold after 12 hours of treatment. A vertical line in Figure 6B was drawn as a point of reference defining the lower limit of NAD(P)H levels in the main population of untreated cells. The electron micrographs taken together with the increase in MTG staining suggest that after TNF+Act D exposure, the mass of individual mitochondria increased, without apparent change to the total number of mitochondria.

We next determined whether TNF+Act D stimulated the release of cytochrome C into the cytosolic fraction of AML12 cells. In untreated cells, very little cytosolic cytochrome C was detected by immunoblot (Figure 6C). After 6 hours of TNF+Act D treatment, cytochrome C was detected in the cytosol and increased up to 18 hours. The release of mitochondrial cytochrome C was also detected by immunofluorescent staining of treated and fixed AML12 cells with an anti-cytochrome C antibody (data not shown). The time course of cytochrome C release from mitochondria is consistent with the timing of caspase-9 activation (Figure 3A), thought to be dependent on release of cytochrome C.

Confocal imaging of NAD(P)H (Figure 7A), $\Delta\psi$m (Figure 7B) and mitochondrial mass (Figure 7C) of living cells corroborated the flow cytometric data shown above. A single field is displayed in Figure 7, A–C, and the three fields are merged in Figure 7D, to illustrate cells in the various stages of apoptosis after TNF+Act D treatment for 12 hours. Nonapoptotic cells are indicated by a star. Early apoptotic cells (reduced mitochondrial $\Delta\psi$m but no apparent morphological changes) are indicated by arrows. The arrowheads point to two cells with morphological changes of apoptosis. Nonapoptotic cells (star), retained high levels of reducing equivalents (purple, Figure 7A) and high mitochondrial membrane potential (orange, Figure 7B) with no change in mitochondrial mass (Figure 7C) resulting in magenta-colored cells in the merged image (Figure 7D). Three early apoptotic cells, indicated by arrows, had low NAD(P)H (Figure 7A) and low $\Delta\psi$m (Figure 7B) but no detectable increase in mitochondrial mass (Figure 7C). In the merged image these cells are seen as orange (Figure 7D). Frankly apoptotic cells are bright green in the merged image (Figure 7D) which reflects the loss of NAD(P)H (Figure 7A), low $\Delta\psi$m (Figure 7B), and increased in mitochondrial mass (Figure 7C). The increased mitochondrial mass coincided with known morphological changes, such as membrane blebbing, which is seen in the green cell in the lower right hand corner.

GSH Depletion Increases ROS Accumulation and Sensitizes Hepatocytes to TNF-Induced Apoptosis

The results shown so far suggest that either increases in mitochondrial generated oxidant stress or loss of cellular antioxidant defense mechanisms (or both) plays a key role in hepatocyte apoptosis. To determine whether ROS were detectable in TNF-treated cells, we used flow cytometric assessment of H2CMX, a nonfluorescent compound which becomes fluorescent when oxidized. In AML12 cells exposed to TNF, no changes in ROS levels were detected (Figure 8A). If, however, cells were pretreated with DEM to acutely deplete cellular GSH levels and then exposed to TNF, the combined treatment resulted in a 70% decrease in GSH levels and a 55% increase in ROS levels (Figure 8A). DEM treatment alone decreased GSH by more than 50% with no increase in ROS. The data demonstrate that ROS accumulate in TNF-treated hepatocytes only after partial depletion of GSH.

Given these results, we examined whether TNF as a single agent would have an apoptotic effect in cells with low levels of cellular GSH. For these experiments AML12 hepatocytes were treated with DEM to acutely deplete GSH as well as with BSO, an inhibitor of γ-glutamyl cysteine synthetase (γ-GCS) activity, to block *de novo* GSH synthesis.[56] As expected, exposure of the cells to TNF alone caused no apoptosis. In contrast, ~45% of cells were apoptotic after combined exposure to TNF, BSO, and DEM (Figure 8B) demonstrating that TNF, which

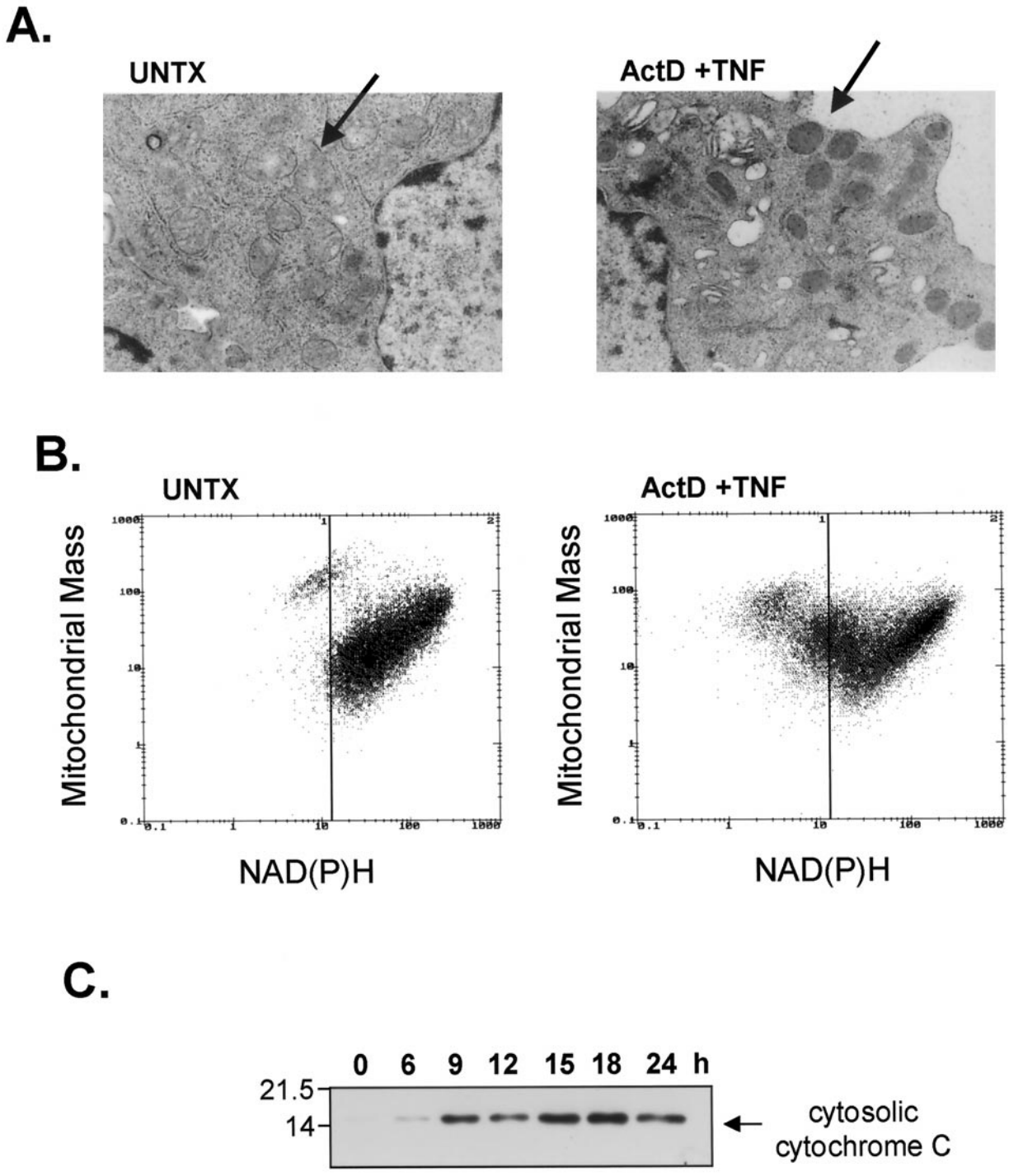

Figure 6. Changes in mitochondrial mass and release of cytochrome C in cells undergoing apoptosis. Cells were treated with TNF+Act D and harvested at 12 hours for transmission electron microscopy, flow cytometry, and immunoblot analysis as described in Materials and Methods. **A:** Mitochondrial condensation as detected by transmission electron microscopy. Electron micrographs from UNTX- and TNF+Act D-treated cells (×12,000). The **arrow** indicates normal mitochondria with visible cristae and normal matrix density in UNTX samples. In the treated samples, the **arrow** indicates condensed mitochondria with increased electron density that obscures the cristae structure. **B:** Bivariate dot-plots of mitochondrial protein (MTG staining) and NAD(P)H from untreated (UNTX) cultures or cultures exposed to TNF+Act D. **C:** Time course of the release of cytosolic cytochrome C after treatment with TNF+Act D. Molecular weight markers are indicated on the left.

does not normally cause cell death in hepatocytes, is an apoptotic agent for hepatocytes with low GSH content. Treatment of cells with both BSO and DEM in the absence of TNF also increased apoptosis in AML12 cells (Figure 8B), demonstrating that a basal level of oxidative stress may be present in these cells which becomes apparent if GSH is depleted.

α-LA is a potent antioxidant capable of protecting GSH levels in injured cells.[57] α-LA functions through multiple activities including direct reduction of oxidized glutathi-

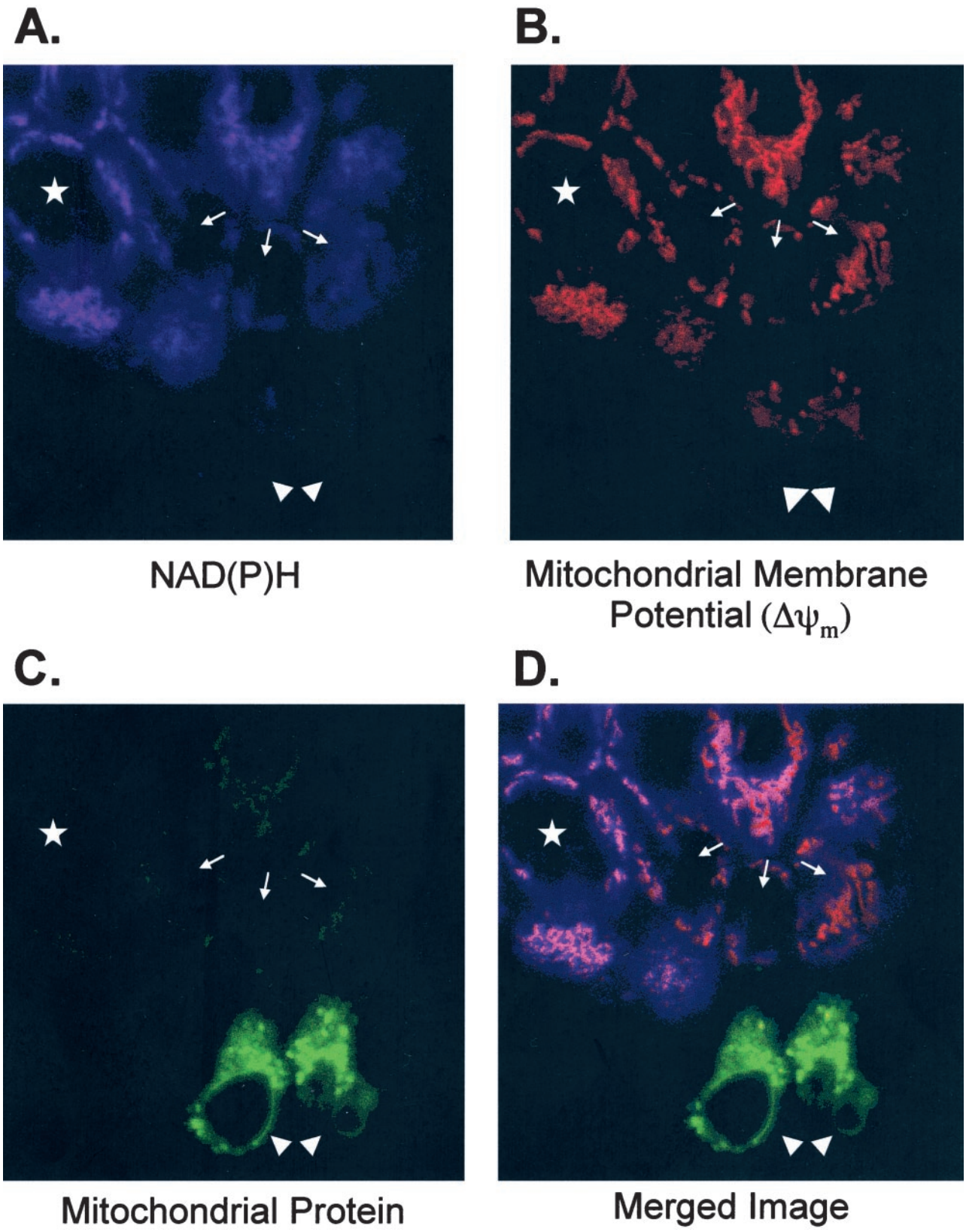

Figure 7. Confocal imaging of AML12 cells undergoing apoptosis. Cells were grown on coverslips and NAD(P)H fluorescence (**A**), mitochondrial membrane potential (CMX staining) (**B**), and mitochondrial mass (MTG) (**C**) were examined as described in Materials and Methods. A single field is shown in **A–C** and the images were merged in (**D**). The field displayed represents the spectrum of changes observed from early to late apoptosis: apparently normal cells (**star**); cells with decrease NAD(P)H but normal $\Delta\Psi$m (**arrows**); frankly apoptotic cells (**arrowheads**).

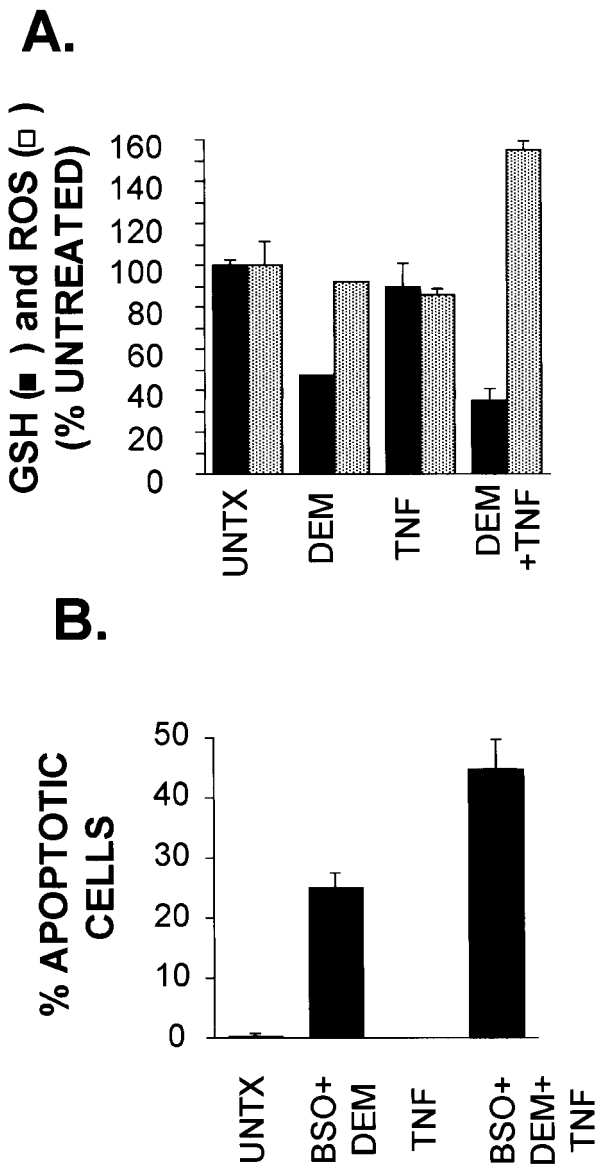

Figure 8. ROS detection and TNF-induced apoptosis in cells with low GSH content. **A:** TNF-induced production of ROS in hepatocytes with low GSH. Cultures were untreated, treated with DEM (0.8 mmol/L), TNF (20 ng/ml), or both DEM and TNF. DEM exposure was for 60 minutes before TNF addition. Cells were harvested 18 hours later for flow cytometry using MCB staining (for GSH) and H2-CMXROS (for measuring ROS). The data are expressed relative to values of untreated samples (UNTX). Error bars represent SEM of triplicate samples. **B:** TNF promotes apoptosis in cells with low GSH. Cultures were left untreated (UNTX) or were treated with TNF (20 ng/ml), BSO (1 mmol/L) + DEM (0.8 mmol/L), or with a combination of BSO+DEM+TNF. Exposure to BSO and DEM started 60 minutes and 30 minutes, respectively, before TNF treatment. Cells were harvested 19 hours later, fixed in 70% ethanol after trypsinization, and stained with DAPI for fluorescence microscopy analysis. Error bars represent SEM from triplicate samples. Data shown are representative of at least three independent experiments.

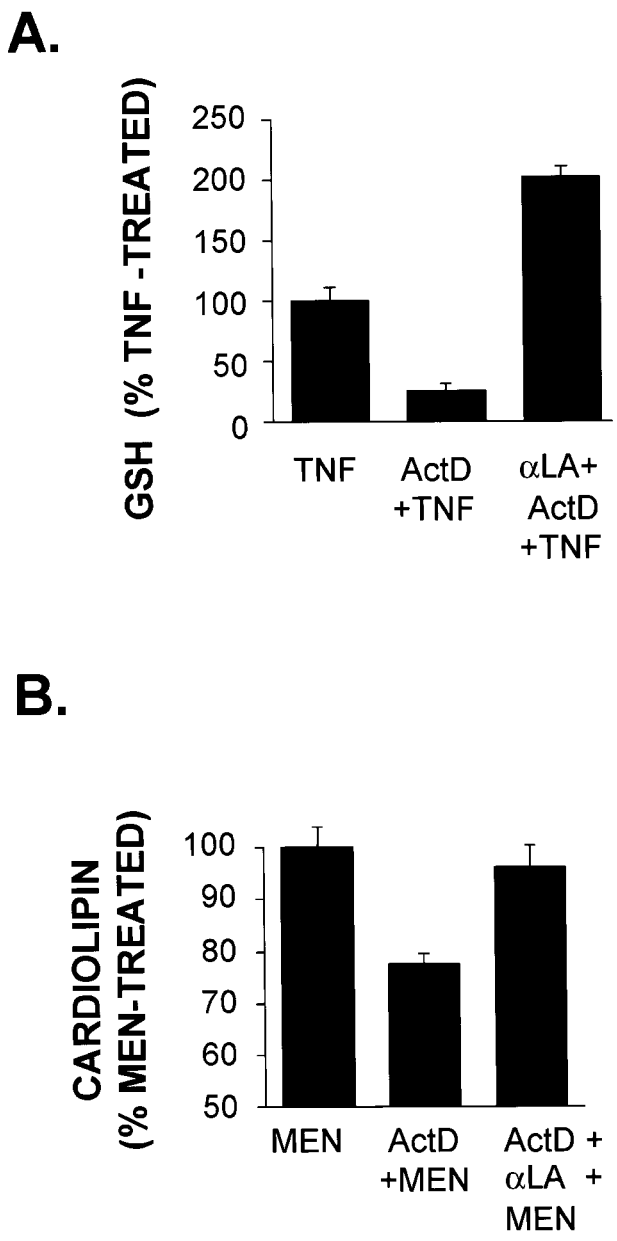

Figure 9. α-Lipoic acid increases GSH levels and prevents injury from oxidative agents. **A:** α-LA blocks the loss of GSH induced by TNF+Act D. Cells were treated with TNF, TNF+Act D, or pretreated with 1 mmol/L α-LA for 60 minutes before the addition of TNF (20 ng/ml) plus Act D (200 nmol/L). After a 12-hour incubation, cells were harvested and cellular GSH content was assessed by flow cytometry using MCB staining as described in Materials and Methods. Error bars represent SEM from triplicate samples. **B:** Act D potentiates cardiolipin loss. Cells were pretreated with Act D (200 nmol/L) alone or together with α-LA (1 mmol/L) for 9 hours. MEN (100 μmol/L) was then added for 3 hours. Cells were harvested and mitochondrial cardiolipin was assessed by flow cytometry using NAO staining as described in Materials and Methods. The error bars represent SEM of triplicate samples relative to menadione-treated cells. MEN treatment resulted in minimal loss of cardiolipin. Data shown are representative of at least three independent experiments.

one, scavenging ROS, chelating metals, reducing oxidized vitamin E and C, as well as stimulating *de novo* synthesis of GSH by maximizing cysteine flow to maintain optimal activity of γGCS, the rate limiting enzymatic step in GSH biosynthesis.[58,59] Figure 9A shows that α-LA not only prevented the decrease in GSH caused by TNF+Act D treatment, but actually increased the GSH content of these cells. These results indicate α-LA may be effective in blocking cell injury caused by a known oxidative agent. MEN is an oxidant that acts by generating mitochondrial ROS.[60] Mitochondrial injury (as assessed by flow cytometric determination of cardiolipin) was detected in cells pretreated with Act D and exposed to MEN for 3 hours.

These cells had cardiolipin levels that were ~25% lower than those cells exposed to MEN alone (Figure 9B) but treatment of cultures with α-LA completely prevented this decrease. These results demonstrate that α-LA can block the damaging effects caused by mitochondrial-generated ROS. Moreover, they imply that injury may result from blockage by Act D of cellular antioxidant defenses involving GSH homeostasis in cells pretreated with Act D and then exposed to either TNF or MEN.

α-LA Acid and a Caspase Inhibitor Prevent Mitochondrial Damage and TNF-Induced Apoptosis

Data presented above demonstrated that α-LA maintains GSH levels in cells treated with TNF+Act D and prevents mitochondrial damage caused by the oxidizing drug MEN. We then determined whether α-LA would prevent apoptosis in AML12 cells exposed to TNF+Act D. The general caspase inhibitor, zVAD-FMK that has previously been shown to inhibit apoptosis in many cell types, was used for comparison. Although 60% of cells were apoptotic as measured by DAPI staining after 15 hours of exposure to TNF+Act D, apoptosis was detectable in only 5% of cells pretreated with zVAD-FMK (Figure 10A). Remarkably, α-LA was as effective as the caspase inhibitor in blocking apoptosis in cells treated with TNF+Act D (Figure 10A). Both zVAD and α-LA also prevented the loss of cardiolipin in cells treated with TNF+Act D (Figure 10B). Moreover, α-LA inhibited the activation of caspase-3 activity (Figure 10C). Caspase-8 and -9 activities were also inhibited by α-LA 12 hours after treatment with TNF+Act D (data not shown). The inset in Figure 10C shows that α-LA inhibited the release of cytochrome C to the cytosol. Thus the antioxidant α-LA prevents mitochondrial damage, caspase activation, and apoptosis in hepatocytes exposed to TNF+Act D reinforcing the notion that oxidative stress is essential for the development of apoptosis in this system. It is of interest to note that α-LA inhibits TNF-induced NFκB activation[57] and on the basis of this effect might have been expected to enhance rather than prevent apoptosis.

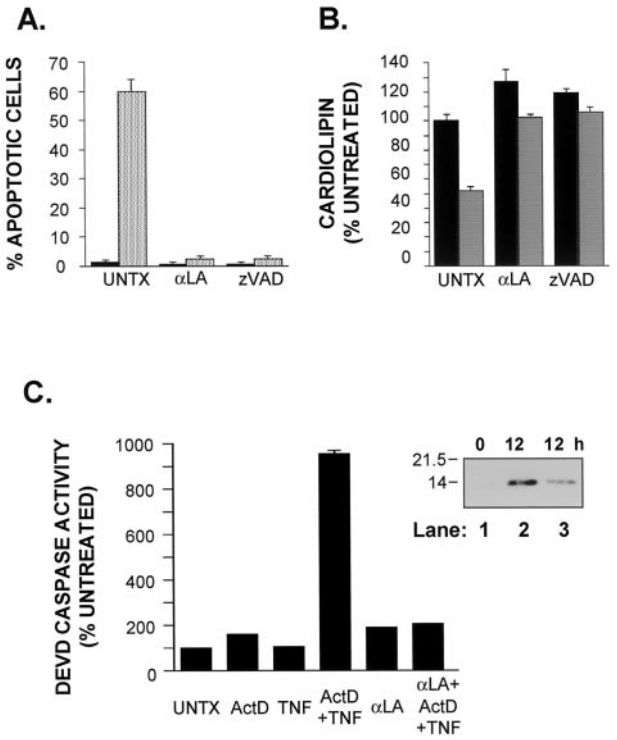

Figure 10. α-LA and a caspase inhibitor block TNF-induced mitochondrial injury and apoptosis. Cells were pretreated with zVAD-FMK (100 μmol/L) for 3 hours or α-LA (1 mmol/L) for 1 hour before the addition of TNF+Act D as described in Materials and Methods. **A:** Both α-LA and zVAD-FMK block apoptosis induced by TNF+Act D treatment. Cells were harvested 18 hours after the addition of TNF, fixed in 70% ETOH, and stained with DAPI as described in Materials and Methods. Error bars represent SEM of triplicate plates. UNTX, **black bars** and TNF+Act D treated, **stippled bars**. **B:** Both α-LA and zVAD-FMK block loss of cardiolipin induced by TNF+Act D treatment. Cells were harvested 12 hours after the addition of TNF and analyzed by flow cytometry using NAO staining as described in Materials and Methods. Error bars represent SEM of triplicate plates. UNTX, **black bars** and TNF+Act D treated, **stippled bars**. Values are normalized to UNTX samples. **C:** Both α-LA and zVAD-FMK block caspase-3 activity induced by TNF+Act D treatment. Cells were harvested 15 hours after the addition of TNF and analyzed for caspase-3 activity as described in Materials and Methods. Error bars represent SEM of triplicate plates. Values are normalized to untreated samples. Data shown are representative of at least three independent experiments. **Inset:** TNF+Act D-induced cytosolic cytochrome C release is blocked by α-LA. Cells were harvested 12 hours after the addition of TNF and release of cytosolic cytochrome C was detected by immunoblot analysis as described in Materials and Methods. Protein from untreated cells, cells treated with TNF+Act D for 12 hours, and cells pretreated with α-LA and then treated with TNF+Act D for 12 hours are shown in **lanes 1**, **2**, and **3**, respectively.

Discussion

TNF can initiate apoptosis, cell proliferation, and the acute phase response in the liver. The goal of this work was to investigate the mechanisms by which TNF causes apoptosis in hepatocytes. AML12 hepatocytes are resistant to TNF-induced cell death, but can be sensitized to undergo apoptosis if exposed to TNF in conjunction with Act D, as is the case for murine hepatocytes *in vivo*. Treatment with TNF+Act D caused oxidative stress as demonstrated by a decrease in NAD(P)H and GSH. The extent of apoptosis in AML12 hepatocytes was exquisitely sensitive to GSH levels as depletion of cellular GSH sensitized cells to TNF-induced apoptosis in the absence of a transcriptional blocking agent. TNF+Act D also induced mitochondrial damage, as shown by decreased transmembrane potential, by losses in cardiolipin content, and by increased mitochondrial condensation and mass.

A salient aspect of this work is the demonstration that TNF by itself can cause apoptosis in GSH-depleted AML12 hepatocytes, a finding that highlights two important observations regarding the mechanisms of TNF-induced apoptosis in hepatocytes. First, oxidative stress and mitochondrial damage play prominent roles in this process and, second, the apoptotic effects of TNF can to a large extent be modulated by the thiol content of the cells. Hepatocytes differ from other cell types such as fibroblasts and lymphocytes, which have been used in many studies on the mechanisms mediating TNF-induced apoptosis, by their very high GSH content, the capacity of the liver to systemically export GSH as well as

the activity of catalase.[23,24] These systems provide hepatocytes with the ability to rapidly and efficiently neutralize the increased ROS produced by TNF. Given the role of GSH as an antioxidant in hepatocytes, it is not entirely surprising that a decrease in the levels of GSH would have a profound effect on apoptosis initiated by oxidant stress. Nevertheless this issue is controversial because some ROS scavenging agents do not effectively block TNF-induced apoptosis in certain cell systems. Free radical scavengers may vary in their protective effect on ROS presumably because of the inability of some agents to partition into the hydrophobic area in which ROS are produced.[2]

The involvement of oxidative stress in mediating TNF-induced apoptosis is further highlighted by the ability of the potent antioxidant, α-LA, to prevent the loss of GSH in cells exposed to TNF+Act D and to completely block caspase activation, mitochondrial damage, cytochrome C release, and apoptosis. Conversely, GSH depletion and inhibition of its *de novo* GSH synthesis sensitized the cells to the cytotoxic effects of TNF given as a single agent. In some cells in culture, increased efflux of GSH has been shown to alter the redox state of the cell without primary involvement of ROS.[61,62] In AML12 hepatocytes, however, the protective effect of α-LA acid suggests that increased ROS drives the consumption of multiple reducing species (NAD(P)H, total cellular thiols, and GSH). Act D sensitization to TNF-mediated cytotoxicity was not specific for this cytokine because Act D also sensitized AML12 cells to the mitochondrial damage caused by the redox cycling agent MEN. Thus, one mechanism by which Act D may sensitize hepatocytes to apoptosis is the blocking of transcription of genes involved in oxidant defenses. A potential target of this effect is γGCS transcription, which in preliminary experiments seems to be decreased after TNF+Act D treatment (data not shown). Glutathione decrease has been considered to be a contributing factor in TNF-induced cell death.[63–65] Mehlen et al[63] showed that proteins such as heat shock protein 27 (hsp27) and alphaB-crystallin provide protection against TNF-induced cell death by raising intracellular GSH. More recently Manna et al[66] demonstrated that overexpression of γGCS protects H4–11E hepatoma cells from TNF-induced cytotoxicity.

Condensed mitochondria with increased folding of the inner membrane and low energy states have been detected at an early stage of mitochondrial injury during apoptosis.[53,54,67] In Colo-205 human colon carcinoma cells, herbimycin-induced apoptosis resulted in condensed mitochondria in which the inner and outer membrane are closely associated and increase in number possibly as a compensatory mechanism.[52] However, these condensed mitochondria have low membrane potential, thus, their proliferation actually contributes to injury. The morphology of condensed mitochondria in AML12 cells was similar to that described in Colo-205 apoptosis induced by herbimycin.[52]

TNF binding to its receptors results in the recruitment of adapter molecules including TRADD and FADD. Engagement of FADD with the receptor complex leads to caspase-8 activation.[1,5] In apoptotic pathways that primarily depend on mitochondrial damage and cytochrome-C release (type II cells), there is a weak, early activation of caspase-8, as well as a late activation believed to be a consequence of caspase-3 and -9 activity.[25,26] The latter condition was observed in our experiments, emphasizing the important role of mitochondria in TNF-induced hepatocyte apoptosis. However, it is difficult to establish a precise sequence of events in AML12 hepatocyte apoptosis because cell death occurred as a nonsynchronized process within a given cell population. Mitochondrial permeability transition, a good marker for apoptotic events, occurs gradually in TNF-induced apoptosis, taking several hours to affect all mitochondria of a single hepatocyte.[16] Although our data suggest that decreased NAD(P)H precedes caspase-3 activation, it is possible that some activation of caspase-3 and -8 may occur before the detection of mitochondrial damage. This is suggested by experiments in which caspase inhibitors blocked not only apoptosis but also the loss of cardiolipin in cells exposed to TNF+Act D. These results imply that early caspase activity during apoptosis in this system may indirectly alter redox homeostatic mechanisms by damaging antioxidant defenses. On the other hand, Bradham et al[16] reported that in rat hepatocytes infected with an adenovirus expressing an IκBα superrepressor, mitochondrial permeability transition in TNF-induced apoptosis is upstream of caspase-3 but downstream of FADD. However, activation of other caspases was not examined in these studies.

It is well known that blockage of NFκB transcriptional activity sensitizes cells to apoptosis induced by TNF.[14] Likewise, it has been suggested that Act D sensitizes cells to TNF-induced apoptosis by inhibiting the expression of anti-apoptotic genes including those regulated by NFκB.[19] However, in AML12 hepatocytes Act D had no effect on TNF-induced NFκB nuclear translocation, DNA EMSA, or transcriptional activity determined by reporter gene assay. However, transcripts of several NFκB target genes were decreased after Act D treatment, such as IκBα and γGCS (data not shown). The possible contribution of NFκB dependent and independent genes to the apoptotic process in AML12 cells is under study.

In summary, we demonstrated that oxidative stress induced by TNF does not produce injury in normal hepatocytes, but causes apoptosis in hepatocytes in which antioxidant defenses are compromised, by Act D or GSH deficiency. Conversely, the antioxidant, α-LA, which prevented the GSH decrease after exposure of cells to TNF+Act D, blocked mitochondrial injury and apoptosis. We conclude that in TNF-induced hepatocyte apoptosis, mitochondrial oxidative injury is a major determinant of cell injury.

Acknowledgments

The assistance of Colin Pritchard, Lisa Prichard, Norbert Deschner, and Priscilla Thurber, and Dr. D. Hockenbery's comments are gratefully acknowledged. We thank the members of the Fausto laboratory for active discussions

and critiques and Matthew Mueller for his help in preparing the manuscript.

References

1. Ashkenazi A, Dixit VM: Death receptors: signaling and modulation. Science 1998, 281:1305–1308
2. Wallach D, Boldin M, Varfolomeev E, Beyaert R, Vandenabeele P, Fiers W: Cell death induction by receptors of the TNF family: towards a molecular understanding. FEBS Lett 1997, 410:96–106
3. Arch RH, Gedrich RW, Thompson CB: Tumor necrosis factor receptor-associated factors (TRAFs): a family of adapter proteins that regulates life and death. Genes Dev 1998, 12:2821–2830
4. Ghosh S, May MJ, Kopp EB. NFκB and Rel proteins: evolutionarily conserved mediators of immune responses. Annu Rev Immunol 1998, 16:225–260
5. Hsu H, Xiong J, Goeddel D: The TNF receptor 1-associated protein TRADD signals cell death and NFκB activation. Cell 1995, 81:495–504
6. Heinrich P, Behrmann I, Graeve L, Grotzinger J, Haan S, Horn F, Horsten U, Kerr I, May P, Muller-Newen G, Schaper F, Terstegen L, Thiel S: The acute-phase response of the liver: molecular mechanism of IL-6 signalling from the plasma membrane to the nucleus. Signalling in the Liver. Edited by D Haussinger, P Heinrich. Dordrecht, Kluwer Academic Publishers, 1998, pp 55–71
7. Akerman P, Cote P, Yang SQ, McClain C, Nelson S, Bagby GJ, Diehl AM: Antibodies to tumor necrosis factor-alpha inhibit liver regeneration after partial hepatectomy. Am J Physiol 1992, 263:G579–G585
8. Yamada Y, Kirillova I, Peschon JJ, Fausto N: Initiation of liver growth by tumor necrosis factor: deficient liver regeneration in mice lacking type I tumor necrosis factor receptor. Proc Natl Acad Sci USA 1997, 94:1441–1446
9. Yamada Y, Fausto N: Deficient liver regeneration after carbon tetrachloride injury in mice lacking type 1 but not type 2 tumor necrosis factor receptor. Am J Pathol 1998, 152:1577–1589
10. Yamada Y, Webber EM, Kirillova I, Peschon JJ, Fausto N: Analysis of liver regeneration in mice lacking type 1 or type 2 tumor necrosis factor receptor: requirement for type 1 but not type 2 receptor. Hepatology 1998, 28:959–970
11. Colell A, Garcia-Ruiz C, Miranda M, Ardite E, Mari M, Morales A, Corrales F, Kaplowitz N, Fernandez-Checa JC: Selective glutathione depletion of mitochondria by ethanol sensitizes hepatocytes to tumor necrosis factor. Gastroenterology 1998, 115:1541–1551
12. Faubion WA, Gores GJ: Death receptors in liver biology and pathobiology. Hepatology 1999, 29:1–4
13. Leist M, Gantner F, Bohlinger I, Germann PG, Tiegs G, Wendel A: Murine hepatocyte apoptosis induced in vitro and in vivo by TNF-alpha requires transcriptional arrest. J Immunol 1994, 153:1778–1788
14. Leist M, Gantner F, Kunstle G, Wendel A: Cytokine-mediated hepatic apoptosis. Rev Physiol Biochem Pharmacol 1998, 133:109–155
15. Lemasters JJ, Nieminen AL, Qian T, Trost LC, Elmore SP, Nishimura Y, Crowe RA, Cascio WE, Bradham CA, Brenner DA, Herman B: The mitochondrial permeability transition in cell death: a common mechanism in necrosis, apoptosis and autophagy. Biochim Biophys Acta 1998, 1366:177–196
16. Bradham CA, Qian T, Streetz K, Trautwein C, Brenner DA, Lemasters JJ: The mitochondrial permeability transition is required for tumor necrosis factor alpha-mediated apoptosis and cytochrome c release. Mol Cell Biol 1998, 18:6353–6364
17. Goossens V, Grooten J, De Vos K, Fiers W: Direct evidence for tumor necrosis factor-induced mitochondrial reactive oxygen intermediates and their involvement in cytotoxicity. Proc Natl Acad Sci USA 1995, 92:8115–8119
18. Schulze-Osthoff K, Bakker AC, Vanhaesebroeck B, Beyaert R, Jacob WA, Fiers W: Cytotoxic activity of tumor necrosis factor is mediated by early damage of mitochondrial functions. Evidence for the involvement of mitochondrial radical generation. J Biol Chem 1992, 267: 5317–5323
19. Xu Y, Bialik S, Jones BE, Iimuro Y, Kitsis RN, Srinivasan A, Brenner DA, Czaja MJ: NF-kappaB inactivation converts a hepatocyte cell line TNF-alpha response from proliferation to apoptosis. Am J Physiol 1998, 275:C1058–C1066
20. Qian T, Herman B, Lemasters JJ: The mitochondrial permeability transition mediates both necrotic and apoptotic death of hepatocytes exposed to Br-A23187. Toxicol Appl Pharmacol 1999, 154:117–125
21. Sidoti-de Fraisse C, Rincheval V, Risler Y, Mignotte B, Vayssiere JL: TNF-alpha activates at least two apoptotic signaling cascades. Oncogene 1998, 17:1639–1651
22. Hampton MB, Orrenius S: Dual regulation of caspase activity by hydrogen peroxide: implications for apoptosis. FEBS Lett 1997, 414: 552–556
23. Lu SC: Regulation of hepatic glutathione synthesis. Semin Liver Dis 1998, 18:331–343
24. Fernandez-Checa JC, Kaplowitz N, Garcia-Ruiz C, Colell A: Mitochondrial glutathione: importance and transport. Semin Liver Dis 1998, 18:389–401
25. Scaffidi C, Fulda S, Srinivasan A, Friesen C, Li F, Tomaselli KJ, Debatin KM, Krammer PH, Peter ME: Two CD95 (APO-1/Fas) signaling pathways. Embo J 1998, 17:1675–1687
26. Gross G, McDonnell JM, Korsmeyer SJ: BCL-2 family members and the mitochondria in apoptosis. Genes Dev 1999, 13:1899–1911
27. Wu JC, Merlino G, Fausto N: Establishment and characterization of differentiated, nontransformed hepatocyte cell lines derived from mice transgenic for transforming growth factor alpha. Proc Natl Acad Sci USA 1994, 91:674–678
28. FitzGerald MJ, Webber EM, Donovan JR, Fausto N: Rapid DNA binding by nuclear factor kappa B in hepatocytes at the start of liver regeneration. Cell Growth Differ 1995, 6:417–427
29. Ghibelli L, Coppola S, Fanelli C, Rotilio G, Civitareale P, Scovassi AI, Ciriolo MR: Glutathione depletion causes cytochrome c release even in the absence of cell commitment to apoptosis. FASEB J 1999, 13:2031–2036
30. Berberich I, Shu GL, Clark EA. Cross-linking CD40 on B cells rapidly activates nuclear factor-kappa B: J Immunol 1994, 153:4357–4366
31. Poot M, Pierce RH: Detection of changes in mitochondrial function during apoptosis by simultaneous staining with multiple fluorescent dyes and correlated multiparameter flow cytometry. Cytometry 1999, 35:311–317
32. Poot M, Verkerk A, Koster JF, Jongkind JF: De novo synthesis of glutathione in human fibroblasts during in vitro ageing and in some metabolic diseases as measured by a flow cytometric method. Biochim Biophys Acta 1986, 883:580–584
33. Hedley DW, Chow S: Evaluation of methods for measuring cellular glutathione content using flow cytometry. Cytometry 1994, 15:349–358
34. Hotz MA, Gong J, Traganos F, Darzynkiewicz Z: Flow cytometric detection of apoptosis: comparison of the assays of in situ DNA degradation and chromatin changes. Cytometry 1994, 15:237–244
35. Van Antwerp DJ, Martin SJ, Verma IM, Green DR: Inhibition of TNF-induced apoptosis by NF-kappa B. Trends Cell Biol 1998, 8:107–111
36. Iimuro Y, Nishiura T, Hellerbrand C, Behrns KE, Schoonhoven R, Grisham JW, Brenner, DA. NFkappaB prevents apoptosis and liver dysfunction during liver regeneration: J Clin Invest 1998, 101:802–811
37. Wu M, Lee H, Bellas RE, Schauer SL, Arsura M, Katz D, FitzGerald MJ, Rothstein TL, Sherr DH, Sonenshein GE: Inhibition of NF-kappaB/Rel induces apoptosis of murine B cells. EMBO J 1996, 15:4682–4690
38. Doi TS, Marino MW, Takahashi T, Yoshida T, Sakakura T, Old LJ, Obata Y: Absence of tumor necrosis factor rescues RelA-deficient mice from embryonic lethality. Proc Natl Acad Sci USA 1999, 96: 2994–2999
39. Rosenfeld M, Prichard L, Shiojiri N, Fausto N: Lack of signaling through tumor necrosis factor receptor type 1 (TNFR-1) rescues the embryonic lethal phenotype of RelA knockout mice. Am J Pathol 2000, 156:997–1007
40. Bellas RE, FitzGerald MJ, Fausto N, Sonenshein GE: Inhibition of NF-kappa B activity induces apoptosis in murine hepatocytes. Am J Pathol 1997, 151:891–896
41. Arsura M, FitzGerald MJ, Fausto N, Sonenshein GE: Nuclear factor-kappaB/Rel blocks transforming growth factor beta1-induced apoptosis of murine hepatocyte cell lines. Cell Growth Differ 1997, 8:1049–1059

42. Baldwin AS Jr: The NF-kappa B and I kappa B proteins: new discoveries and insights. Annu Rev Immunol 1996, 14:649–683
43. Cressman DE, Greenbaum LE, DeAngelis RA, Ciliberto G, Furth EE, Poli V, Taub R: Liver failure and defective hepatocyte regeneration in interleukin-6-deficient mice. Science 1996, 274:1379–1383
44. Kirillova I, Chaisson M, Fausto N: Tumor necrosis factor induces DNA replication in hepatic cells through nuclear factor κB activation. Cell Growth Differ 1999, 10:819–828
45. Libermann TA, Baltimore D: Activation of interleukin-6 gene expression through the NFκB transcription factor. Mol Cell Biol 1990, 10: 2327–2334
46. Lu SC: Regulation of hepatic glutathione synthesis: current concepts and controversies. FASEB J 1999, 13:1169–1183
47. Shidoji Y, Hayashi K, Komura S, Ohishi N, Yagi K: Loss of molecular interaction between cytochrome c and cardiolipin due to lipid peroxidation. Biochem Biophys Res Commun 1999, 264:343–347
48. McAuley KE, Fyfe PK, Ridge JP, Isaacs NW, Cogdell RJ, Jones MR: Structural details of an interaction between cardiolipin and an integral membrane protein. Proc Natl Acad Sci USA 1999, 96:14706–14711
49. Petit PX, Lecoeur H, Zorn E, Dauguet C, Mignotte B, Gougeon ML: Alterations in mitochondrial structure and function are early events of dexamethasone-induced thymocyte apoptosis. J Cell Biol 1995, 130: 157–167
50. Polyak K, Xia Y, Zweier JL, Kinzler KW, Vogelstein B: A model for p53-induced apoptosis. Nature 1997, 389:300–305
51. Macho A, Castedo M, Marchetti P, Aguilar JJ, Decaudin D, Zamzami N, Girard PM, Uriel J, Kroemer G: Mitochondrial dysfunctions in circulating T lymphocytes from human immunodeficiency virus-1 carriers. Blood 1995, 86:2481–2487
52. Mancini M, Anderson BO, Caldwell E, Sedghinasab M, Paty PB, Hockenbery DM: Mitochondrial proliferation and paradoxical membrane depolarization during terminal differentiation and apoptosis in a human colon carcinoma cell line. J Cell Biol 1997, 138:449–469
53. Dinsdale D, Zhuang J, Cohen GM: Redistribution of cytochrome c precedes the caspase-dependent formation of ultracondensed mitochondria, with a reduced inner membrane potential, in apoptotic monocytes. Am J Pathol 1999, 155:607–618
54. Jia L, Dourmashkin RR, Newland AC, Kelsey SM: Mitochondrial ultracondensation, but not swelling, is involved in TNF alpha-induced apoptosis in human T-lymphoblastic leukaemic cells. Leuk Res 1997, 21:973–983
55. Metivier D, Dallaporta B, Zamzami N, Larochette N, Susin SA, Marzo I, Kroemer G: Cytofluorometric detection of mitochondrial alterations in early CD95/Fas/APO-1-triggered apoptosis of Jurkat T lymphoma cells. Comparison of seven mitochondrion-specific fluorochromes. Immunol Lett 1998, 61:157–163
56. Meister A: Glutathione deficiency produced by inhibition of its synthesis, and its reversal; applications in research and therapy. Pharmacol Ther 1991, 51:155–194
57. Packer L, Witt EH, Tritschler, HJ: Alpha-lipoic acid as a biological antioxidant: Free Radic Biol Med 1995, 19:227–250
58. Han D, Handelman G, Marcocci L, Sen CK, Roy S, Kobuchi H, Tritschler HJ, Flohe L, Packer L: Lipoic acid increases de novo synthesis of cellular glutathione by improving cystine utilization. Biofactors 1997, 6:321–338
59. Biewenga GP, Haenen GR, Bast A: The pharmacology of the antioxidant lipoic acid. Gen Pharmacol 1997, 29:315–331
60. Thor H, Smith MT, Hartzell P, Bellomo G, Jewell SA, Orrenius S: The metabolism of menadione (2-methyl-1,4-naphthoquinone) by isolated hepatocytes. A study of the implications of oxidative stress in intact cells. J Biol Chem 1982, 257:12419–12425
61. Ghibelli L, Fanelli C, Rotilio G, Lafavia E, Coppola S, Colussi C, Civitareale P, Ciriolo MR: Rescue of cells from apoptosis by inhibition of active GSH extrusion. FASEB J 1998, 12:479–486
62. van den Dobbelsteen DJ, Nobel CSI, Schlegel J, Cotgreave IA, Orrenius S, Slater AF: Rapid and specific efflux of reduced glutathione during apoptosis induced by anti-Fas/APO-1 antibody. J Biol Chem 1996, 271:15420–15427
63. Mehlen P, Kretz-Remy C, Preville X, Arrigo AP: Human hsp27, Drosophila hsp27 and human alphaB-crystallin expression-mediated increase in glutathione is essential for the protective activity of these proteins against TNFalpha-induced cell death. Embo J 1996, 15: 2695–2706
64. Shoji Y, Uedono Y, Ishikura H, Takeyama N, Tanaka T: DNA damage induced by tumour necrosis factor-alpha in L929 cells is mediated by mitochondrial oxygen radical formation. Immunology 1995, 84:543–548
65. Fernandez-Checa JC, Garcia-Ruiz C, Colell A, Morales A, Mari M, Miranda M, Ardite E: Oxidative stress: role of mitochondria and protection by glutathione. Biofactors 1998, 8:7–11
66. Manna SK, Kuo MT, Aggarwal BB: Overexpression of gamma-glutamylcysteine synthetase suppresses tumor necrosis factor-induced apoptosis and activation of nuclear transcription factor-kappa B and activator protein-1. Oncogene 1999, 18:4371–4382
67. James TN, Terasaki F, Pavlovich ER, Vikhert AM: Apoptosis and pleomorphic micromitochondriosis in the sinus nodes surgically excised from five patients with the long QT syndrome. J Lab Clin Med 1993, 122:309–323